Clin Orthop Relat Res
DOI 10.1007/s11999-013-2788-y

Clinical Orthopaedics and Related Research®
A Publication of The Association of Bone and Joint Surgeons®

SYMPOSIUM: PAPERS PRESENTED AT THE ANNUAL MEETINGS OF THE HIP SOCIETY

MRI Predicts ALVAL and Tissue Damage in Metal-on-Metal Hip Arthroplasty

Danyal H. Nawabi MD, FRCS(Orth), Stephanie Gold BA, Steven Lyman PhD, Kara Fields MS, Douglas E. Padgett MD, Hollis G. Potter MD

Abstract

Background Adverse local tissue reactions (ALTR) around metal-on-metal (MOM) hip arthroplasties are increasingly being recognized as a cause of failure. These reactions may be associated with intraoperative tissue damage and complication rates as high as 50% after revision. Although MRI can identify ALTR in MOM hips, it is unclear whether the MRI findings predict those at revision surgery.

Questions/purposes We therefore (1) identified which MRI characteristics correlated with histologically confirmed ALTR (using the aseptic lymphocytic vasculitis-associated lesions [ALVAL] score) and intraoperative tissue damage and (2) developed a predictive model using modified MRI to detect ALVAL and quantify intraoperative tissue damage.

Methods We retrospectively reviewed 68 patients with failed MOM hip arthroplasties who underwent preoperative MRI and subsequent revision surgery. Images were analyzed to determine synovial volume, osteolysis, and synovial thickness. The ALVAL score was used to grade tissue samples, thus identifying a subset of patients with ALTR. Intraoperative tissue damage was graded using a four-point scale. Random forest analysis determined the sensitivity and specificity of MRI characteristics in detecting ALVAL (score $\geq$ 5) and intraoperative tissue damage.

Results Maximal synovial thicknesses and synovial volumes as determined on MRI correlated with the ALVAL score and were higher in cases of severe intraoperative tissue damage. Our MRI predictive model showed sensitivity and specificity of 94% and 87%, respectively, for detecting ALVAL and 90% and 86%, respectively, for quantifying intraoperative tissue damage.

The institution of one or more of the authors (HGP) has received, during the study period, funding from General Electric Healthcare (Waukesha, WI, USA). One of the authors certifies that he (DEP), or a member of his or her immediate family, has or may receive payments or benefits, during the study period, an amount less than $10,000 from Stryker (Mahwah, NJ, USA), and an amount of $10,000–$100,000 from Mako (Fort Lauderdale, FL, USA).
All ICMJE Conflict of Interest Forms for authors and *Clinical Orthopaedics and Related Research* editors and board members are on file with the publication and can be viewed on request.
Clinical Orthopaedics and Related Research neither advocates nor endorses the use of any treatment, drug, or device. Readers are encouraged to always seek additional information, including FDA-approval status, of any drug or device prior to clinical use.
Each author certifies that his or her institution approved the human protocol for this investigation, that all investigations were conducted in conformity with ethical principles of research, and that informed consent for participation in the study was obtained.
This work was performed at Hospital for Special Surgery, New York, NY, USA.

D. H. Nawabi, D. E. Padgett
Adult Reconstruction and Joint Replacement Division Surgery, Hospital for Special Surgery, New York, NY, USA

S. Gold, H. G. Potter (✉)
Department of Radiology and Imaging, Hospital for Special Surgery, 535 East 70th Street, New York, NY 10021, USA
e-mail: potterh@hss.edu

S. Lyman, K. Fields
Epidemiology and Biostatistics Core, Hospital for Special Surgery, New York, NY, USA

S. Lyman, D. E. Padgett, H. G. Potter
Weill Cornell Medical College of Cornell University, New York, NY, USA

Published online: 26 January 2013

Conclusions MRI is sensitive and specific in detecting ALVAL and tissue damage in patients with MOM hip implants. MRI can be used as a screening tool to guide surgeons toward timely revision surgery.
Level of Evidence Level III, diagnostic study. See Guidelines for Authors for a complete description of levels of evidence.

Introduction

The current generation of metal-on-metal (MOM) cobalt-chromium-molybdenum bearings in hip arthroplasty have shown overall survivorship rates at 5 and 10 years of 98% and 94% [3, 4, 13, 18, 31] respectively. However, reports have emerged describing the presence of periprosthetic soft tissue lesions, which have been described interchangeably as adverse local tissue reactions (ALTR) [1], adverse reactions to metal debris (ARMD) [17], aseptic lymphocytic vasculitis-associated lesions (ALVAL) [33], metallosis [23], and pseudotumors [24]. Although these soft tissue masses are not malignant or infectious, they can be associated with catastrophic local tissue destruction [24] and complication rates of 50% after revision arthroplasty [6]. The importance of early detection and prompt revision therefore is paramount.

Histologically, the soft tissue lesions are characterized by lymphocytes, histiocytes, and necrosis [33] but also may exhibit metallic deposits and corrosion products [20]. Campbell et al. [2] proposed a histologic scoring system which predicts the presence of a lymphocyte-predominant reaction in the soft tissues, known as ALVAL. This is believed to reflect a type IV hypersensitivity reaction [33] that typically is either absent or low grade in patients with excess metal wear [2, 17]. Schmalzried [28] first proposed the term ALTR to include all adverse responses resulting from wear-related and biologic causes. ALTR has since been used by others [1] and we have also used ALTR as an encompassing term to describe all failures secondary to periprosthetic soft tissue lesions, regardless whether attributable to excess metal wear.

Several recent studies suggest ALTR can occur in asymptomatic, well-functioning MOM hip arthroplasties [15, 22, 34] and that its prevalence is similar in patients who are asymptomatic and patients with painful MOM hip implants [10]. These studies used either ultrasonography or metal artifact reduction sequence (MARS) MRI to detect ALTR but did not find objective differences in the MRI characteristics between well-functioning and failing hips.

With the emphasis on early revision surgery in cases of ALTR, the use of MRI in identifying a failing MOM hip implant warrants investigation. MARS MRI is recognized as a useful modality in the assessment of ALTR around MOM hip implants, showing characteristics such as size, shape, and contents of lesions [10, 11, 27]. Newer prototype pulse sequences are available that improve observation of soft tissue around MOM hip implants [12]. However, it is unclear whether these MRI characteristics correspond to ALTR that may result in substantial intraoperative tissue damage. We sought to use this technology to study the potential of modified MRI to detect a specific subset of ALTR and intraoperative tissue damage as early as possible.

We therefore (1) identified which MRI characteristics correlated with a histologically proven ALTR (using the ALVAL score) and intraoperative tissue damage and (2) developed a predictive model using modified MRI to detect ALVAL and quantify intraoperative tissue damage.

Patients and Methods

From an institutional database we identified 68 patients (70 hips) who had undergone preoperative modified MRI followed by revision surgery for a failed MOM hip arthroplasty. As part of an ongoing institutional initiative, all patients with a MOM hip arthroplasty presenting with pain and/or functional impairment were recommended to undergo modified MRI. There were 31 males and 37 females with a median age of 52 and 57 years, respectively, at the time of primary surgery. The median time to revision was 36 months (range, 11–103 months). All methods were approved by our institutional review board and informed consent was obtained from all patients before enrollment in the study.

The hips were revised by 13 surgeons at our institution. Twenty-one (30%) of the primary hip arthroplasties were performed at our institution and the remainder were performed in other centers. The reasons for revision were determined according to the categories used by the National Joint Registry for England and Wales [7, 19]. These included aseptic acetabular loosening (n = 8), aseptic femoral loosening (n = 3), component malalignment (n = 4), infection (n = 1), and unexplained pain (n = 54). An infection workup was performed on every patient in this study which included serum C-reactive protein level and if elevated, fluoroscopically guided aspiration of the hip with fluid tested for microbiologic culture and sensitivities. A primary diagnosis was established for all patients with a history, physical examination, and radiographs, except for the patients with component loosening and unexplained pain. Acetabular and femoral loosening was suggested on radiographs but confirmed intraoperatively. Patients with unexplained pain were further investigated with modified MRI. The decision to revise was based primarily on the

presence of pain originating from the hip and/or the presence of a functional impairment. Most recently (since acquisition of the data reported in our study), the presence of an adverse synovial reaction on MRI is taken into consideration when making a decision regarding revision surgery. Forty-six of the 70 hips had large-diameter (> 38 mm) MOM THA implants with monoblock cups. These included 24 ASR (DePuy, Leeds, UK), eight BHR (Smith & Nephew, Memphis, TN, USA), seven M2a-Magnum (Biomet, Warsaw, IN, USA), four Durom (Zimmer, Warsaw, IN, USA), and three Conserve Plus (Wright Medical Technology, Memphis, TN, USA) implants. The remaining 24 hips had hip resurfacings, which included 19 BHR (Smith & Nephew), two Cormet (Corin, Cirencester, UK), one ReCap (Biomet), and two Conserve Plus (Wright Medical Technology) implants.

Intraoperative tissue damage was subjectively graded by the operating surgeon using a four-point scale devised after consultation with two experienced arthroplasty surgeons (DP, DN): Grade 0 = normal tissue; Grade 1 = fluid collection ± mild synovial reaction ± pseudocapsular dehiscence; Grade 2 = Grade 1 + moderate to severe synovial reaction ± metallosis; or Grade 3 = Grade 2 + abductor damage and/or bone loss. A damage score of 2 or greater was considered indicative of severe soft tissue damage. Operative reports were not available for two patients and therefore no intraoperative score could be calculated; these patients were excluded from the final analysis.

All patients underwent preoperative MRI using a standard protocol optimized to reduce metallic susceptibility artifact [25]. Scanning was performed using 1.5-T clinical scanners (GE Healthcare, Waukesha, WI, USA) using either an eight-channel cardiac coil (GE Healthcare) or a three-channel shoulder coil (MedRad, Indianola, PA, USA). Two-dimensional fast spin echo (FSE) images were obtained in three planes using modifications to the pulse parameters to reduce susceptibility artifact. A wider receiver bandwidth and oversampling in the frequency encoding axis were used to increase the strength of the readout gradient [29]; the voxel size was reduced, thereby improving spatial resolution; and the number of signals averaged was increased to increase the signal-to-noise ratio [12]. Multiacquisition variable-resonance image combination (MAVRIC) was used in the coronal plane to reduce susceptibility artifact by combining multiple data sets acquired at frequency bands offset from the center proton frequency [12] (Fig. 1). The specific parameters used are summarized (Table 1). Compared with other MARS techniques, our institutional MARS protocol differs greatly, as instead of T1- or T2-weighted sequences, a moderate echo time proton density sequence is used that is fluid sensitive and can delineate very low signal intensity metallic deposits without the loss of signal-to-noise ratio (SNR). In addition, we add the MAVRIC sequence, typically in the coronal plane. MAVRIC is currently under FDA review and we hope it will be available to all orthopaedic surgeons in the near future.

MR images were evaluated by two musculoskeletal radiologists (HGP, AB) through consensus agreement. One is a senior musculoskeletal radiologist with more than 10 years of experience (HGP) in MRI of arthroplasties; the other is a musculoskeletal radiologist with 8 months of experience (AB). MR images were evaluated for the presence and volume of synovitis and osteolysis. Synovitis was defined as the presence of fluid signal intensity material or solid debris, either contained by the pseudocapsule or communicating with the disrupted pseudocapsule. The synovitis was characterized as (1) solid; (2) fluid; or (3) mixed (solid and fluid) in appearance and the maximal thickness of the synovial lining was measured on axial FSE images. Solid synovitis was denoted by intermediate signal intensity material while pure fluid collections had a signal intensity of free water and mixed synovitis had characteristics of both. Any decompression of synovitis into the trochanteric or iliopsoas bursa also was noted (Fig. 2). Osteolysis was defined by the presence of areas of osseous resorption, appearing as intermediate or low intensity replacing the higher signal intensity intramedullary fat on the intermediate-weighted FSE images (Fig. 3). The volumes of synovitis and osteolysis were calculated using a previously validated method of manual segmentation from the coronal MAVRIC or axial FSE images [26, 32]. The pseudocapsule was evaluated for dehiscence, which was characterized by either anterior or posterior capsular detachment. The presence of extracapsular low signal intensity deposits indicative of metallic debris also was noted. The arthroplasty was evaluated for loosening of the femoral and acetabular components as denoted by circumferential bone resorption surrounding the arthroplasty. The abductor muscles were evaluated for disruption resulting from distension of the pseudocapsule (Fig. 4) Preexisting abductor tears were denoted by abnormal signal and morphologic features of the tendon and when any existing adverse local tissue reaction did not impinge or abut the tendon. Additionally, the obturator, sciatic, and femoral nerves were assessed for neurovascular compression, defined by the loss of normal fat planes surrounding the nerve (Fig. 5). Enlarged lymph nodes were denoted by intermediate signal intensity foci in the corresponding anatomic distributions around the implant. Data were collected on a standard form (Appendix 1).

All tissue samples excised at revision surgery were submitted for histologic examination and were reviewed by one musculoskeletal pathologist (GP). The revision surgeons routinely and consistently sampled tissue from the posterior capsule and inferior neck of the femur. The tissue samples were processed routinely: serially cut to maximize information obtained and stained with hematoxylin and

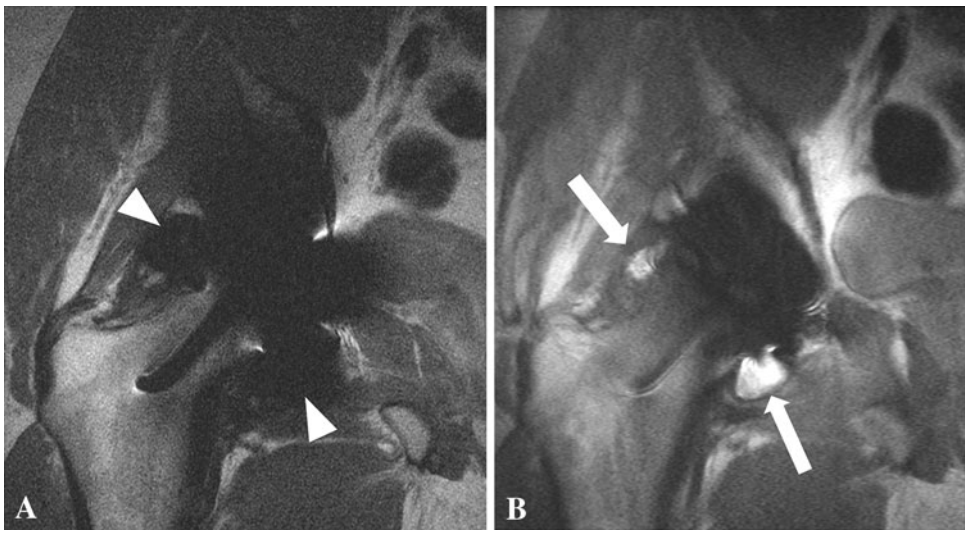

Fig. 1A–B (**A**) The FSE pulse sequence for a 29-year-old man after a right hip resurfacing arthroplasty shows marked susceptibility artifact (white arrowheads) arising from the cobalt-chromium implant, precluding observation of the synovial lining. (**B**) A coronal MAVRIC sequence shows marked reduction in susceptibility artifact, unmasking right hip synovitis (white arrows).

Table 1. Imaging parameters of the hip at 1.5 T in the presence of metal

Parameter	STIR	Axial FSE	Sagittal FSE	Coronal FSE	Coronal MAVRIC
TR (ms)	4500	4500–5000	5500–6500	4500–5500	4000–6000
TE (ms)	18	24–30	25–30	24–34	21–43
TI	150				
RBW (kHz)	83–100	83–100	83–100	83–100	±125
NEX	2	4–5	4–5	4–5	.5
FOV (cm)	Inter-tro	17–19	18–20	18–24	20–24
Matrix	256 × 192	512 × 256	512 × 352	512 × 384	320–512 × 256–384
Slice thickness (mm)/gap	5/0	4/0	3–4/0	4/0	3–4.5/0

STIR = short-tau fast inversion recovery; FSE = fast spin echo; MAVRIC = multiacquisition variable-resonance image combination TR = repetition time; TE = echo time; TI = time to inversion; RBW = receiver bandwidth; NEX = number of excitations FOV = field of view.

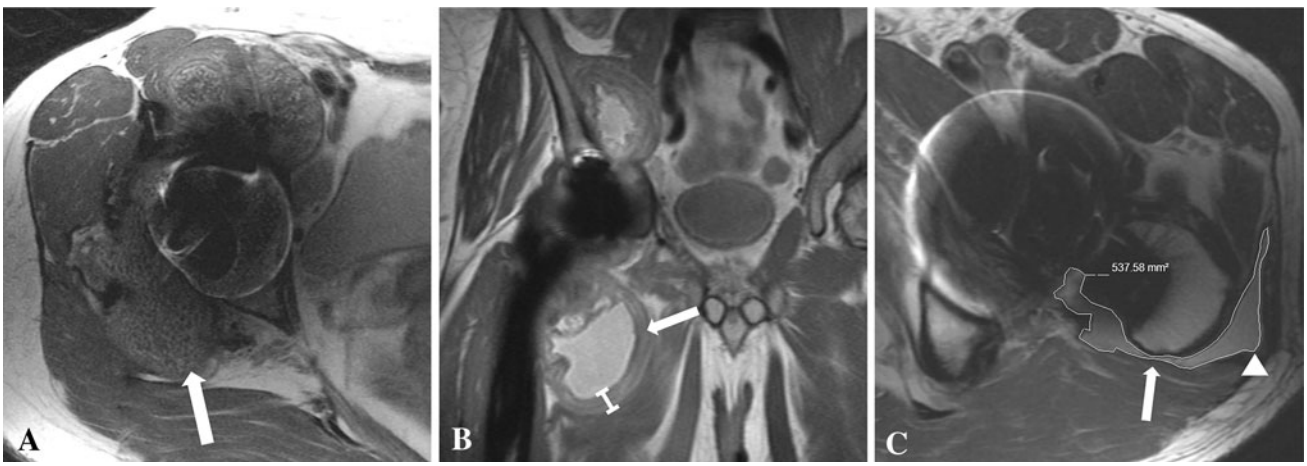

Fig. 2A–C (**A**) An axial FSE image for a 51-year-old woman after right hip resurfacing arthroplasty shows mixed- (fluid and solid) type synovitis (white arrow). (**B**) The coronal MAVRIC prototype sequence for a 57-year-old man after a MOM THA shows marked synovial thickening (white arrow). (**C**) The axial FSE image for a 65-year-old man after his THA shows decompression of synovitis into the greater trochanteric bursa (white arrowhead). There is lateral dehiscence of the posterior pseudocapsule (white arrow). The overlaid graphics show the segmentation method used to quantify the volume of synovitis.

Fig. 3 A coronal MAVRIC prototype pulse sequence for a 52-year-old woman obtained after right hip resurfacing arthroplasty shows extensive replacement of the normal periacetabular marrow fat by low signal intensity (white arrowheads), consistent with osteolysis. There is an adjacent large extracapsular low signal intensity deposit (white arrow) abutting the sciatic nerve.

Fig. 4 A coronal FSE image obtained after a left MOM THA in a 62-year-old man shows decompression of the synovitis into the greater trochanteric bursa with associated disruption of the hip abductors and retraction of the torn tendons (white arrow). Atrophy of the muscle bellies also is evident (black arrow).

eosin. Samples were examined under light microscopy without knowledge of MRI findings. Sections were evaluated for the presence of fibrinous exudates, necrosis, inflammatory cells, metallic deposits, and corrosion products. The status of the synovial lining, inflammatory infiltrate, and tissue organization was recorded to give an ALVAL score from 0 to 10 as proposed by Campbell et al. [2]. In the circumstance where these features could not be delineated reliably owing to widespread necrosis, no score was given. There were four such cases. An ALVAL score of 5 or greater was consistent with a diagnosis of moderate to severe ALVAL [2]. There were four histology samples in which only necrosis was observed, and these therefore were noncontributory to the final analysis.

The first dependent variable considered in this study was whether the patients had ALVAL (ALVAL score ≥ 5). The independent (predictor) variables considered were the MRI characteristics (Appendix 1). The second dependent variable was whether the patients had severe intraoperative tissue damage (damage score ≥ 2). This also was compared with the MRI characteristics (Appendix 1). For both analyses, Fisher's exact test was used to compare categorical independent variables between outcome groups and the Wilcoxon rank-sum test was used to compare continuous independent variables. The Spearman rank correlation coefficient was used to identify correlations between MRI characteristics and the ALVAL and tissue damage scores. Random forest analysis was used to determine which MRI characteristics were most predictive of detecting ALVAL (ALVAL score ≥ 5) and intraoperative tissue damage and to identify the sensitivity and specificity of selected MRI characteristics in detecting ALVAL (ALVAL score ≥ 5) and quantifying intraoperative tissue damage as none to mild (Grades 0–1) or severe (Grades 2–3). A random forest is an ensemble (set) of decision trees, each built from a bootstrap sample of observations. Each decision tree is constructed by sequential partitioning of the sample by the predictor (from a random subset of variables) that allows for the best segregation of outcome groups. The outcome of each observation is predicted by the majority assignment of the ensemble of trees. The relative contribution of each predictor to the forest's predictive ability is reflected by its calculated importance score. Sensitivity, specificity, and predictor importance scores were pooled over 10 forests of 10,000 trees for each of the independent outcomes. Random forest analysis has been used previously in MRI research [21]. All inferential analyses were performed using the SAS System for Windows 9.2 (SAS Institute Inc, Cary, NC, USA). The R party package (R Foundation for Statistical Computing, Vienna, Austria) was used to perform the random forest analysis.

Results

When comparing patients with ALVAL (score ≥ 5) with patients with a low probability of ALVAL (score < 5), the patients with ALVAL were more likely ($p < 0.001$) to have a mixed pattern of synovitis (solid and fluid) with higher

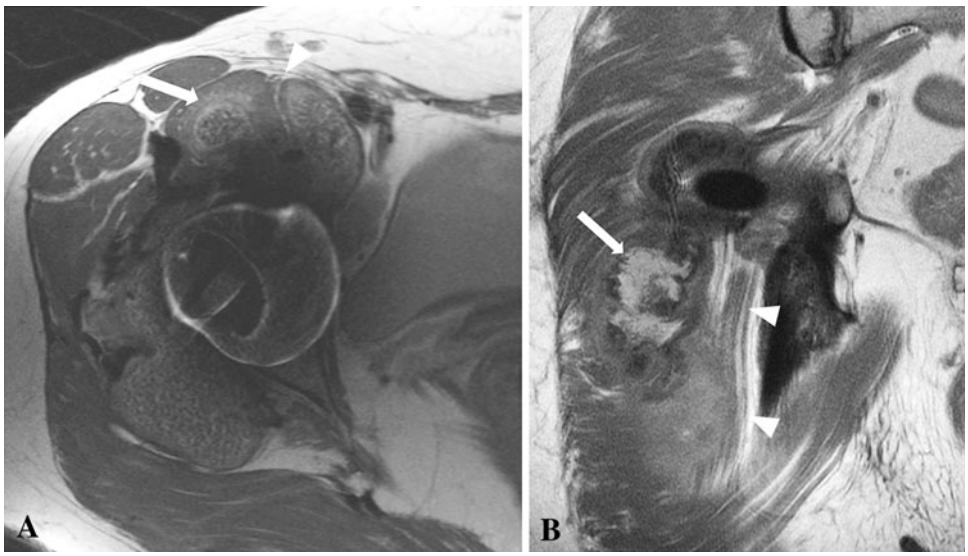

Fig. 5A–B (**A**) An axial FSE image obtained after a right hip resurfacing arthroplasty in a 51-year-old woman shows marked anterior synovial expansion (white arrow) impinging the femoral nerve (white arrowhead). (**B**) The coronal FSE image for a 57-year-old man obtained after a right THA shows marked posterior synovial expansion (white arrow) abutting the adjacent sciatic nerve (white arrowheads).

($p < 0.001$) maximal synovial thicknesses (Fig. 6) and higher ($p < 0.001$) synovial volumes (Fig. 7) as determined on MRI. Decompression of synovitis (Fig. 8), low signal intensity deposits, soft tissue edema, pseudocapsular dehiscence, abductor disruption, and neurovascular compression were more likely to be present on MRI in patients with ALVAL (Table 2). Patients with ALVAL were not more likely to have implant loosening as detected by MRI. Patients with severe tissue damage were more likely ($p < 0.001$) to have a mixed pattern of synovitis with higher ($p < 0.001$) maximal synovial thicknesses and higher ($p < 0.001$) synovial volumes as determined on MRI. Decompression of synovitis, low signal intensity deposits, soft tissue edema, pseudocapsular dehiscence, abductor disruption, and neurovascular compression were more likely to be present on MRI (Table 3) in patients with severe tissue damage (Fig. 9). These patients were not more likely to have implant loosening or the presence of nodes on MRI. Maximal synovial thickness on MRI correlated with ($\rho = 0.81$; 95% CI, 0.70–0.88) the ALVAL score. Synovial volume on MRI also correlated with ($\rho = 0.74$; 95% CI, 0.61–0.84) the ALVAL score.

In our model, maximal synovial thickness was the strongest predictor for the diagnosis of ALVAL. The type and volume of synovitis also were strong predictors of ALVAL. The presence of low signal intensity deposits, osteolysis, and nodes was not indicative of ALVAL (Fig. 10). The presence of pseudocapsular dehiscence, extracapsular synovial decompression, and the type of synovitis were the three strongest predictors of severe intraoperative tissue damage (Fig. 11). Neurovascular compression, soft tissue edema, and the presence of nodes were not suggestive of severe tissue damage. Our MRI predictive model found sensitivity and specificity of 94% and 87%, respectively, for detecting ALVAL and 90% and 86%, respectively, for quantifying intraoperative tissue damage.

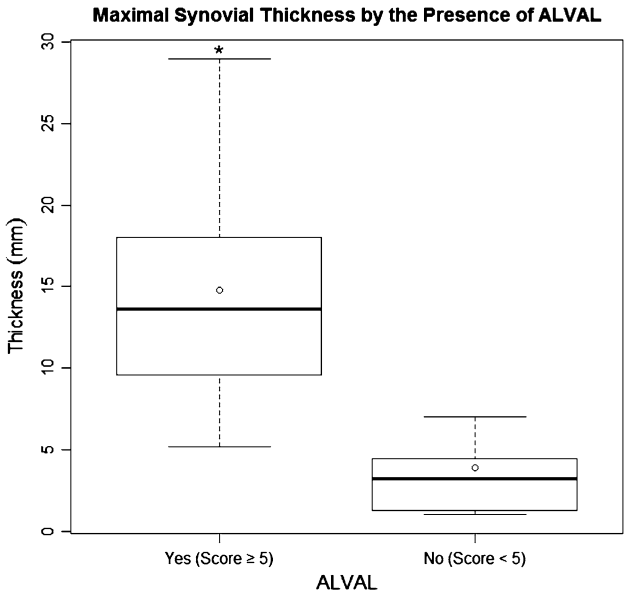

Fig. 6 A box plot shows the interquartile range (box edges representing 25th and 75th percentiles), median (dark bar inside box), and mean (circle) for synovial thickness by the presence of ALVAL. The error bars represent the minimum and maximum observed values within 1.5 times the interquartile range values. Outliers are not shown. The asterisk indicates a major difference in medians between outcome groups.

Discussion

Periprosthetic soft tissue lesions around MOM hip implants have been reported by numerous authors using various terms including ALTR, ARMD, ALVAL, metallosis, and pseudotumor [1, 17, 23, 24, 33]. These soft tissue masses can be associated with major tissue destruction [24] and therefore early recognition and prompt revision are critical. Our aims were to identify which MRI characteristics correlated with the ALVAL score and intraoperative tissue

damage and to develop a predictive model using modified MRI to detect ALVAL as confirmed by histology and to quantify intraoperative tissue damage.

We acknowledge several limitations to our study. First, although we chose the term ALTR to encompass all periprosthetic soft tissue lesions, we only studied a specific subset, namely patients with ALVAL. This was because ALVAL can be confirmed histologically. Therefore, our conclusions on the predictive value of MRI can be applied only to an ALTR occurring secondary to ALVAL. Furthermore, adverse tissue responses secondary to excessive metal wear [14, 16] tend to be histiocyte-dominant with low ALVAL scores [2, 17] and therefore our study design would have clustered these cases in the low-probability ALVAL group. Second, the operating surgeons were blinded to MRI findings and not given any guidance regarding which tissue samples to send for histologic analysis. As a result, there were four samples in which only necrosis was observed, and these therefore were noncontributory to the final analysis. Third, the ALVAL score has been reported to have interobserver and intraobserver variabilities of 0.71 and 0.68, respectively [2]. Our scores are limited by this variability. We addressed this problem by performing the majority of our statistical analyses with ALVAL scores broken into two groups, because the error in grading a tissue sample as ALVAL 5 or greater or less than 5 is subject to less variability. Fourth, we analyzed MOM hip implants from various manufacturers. This could not be avoided because we are a tertiary referral center and 70% of the hips in this study were referred from outside centers. Finally, the intraoperative tissue damage score is subjective and not validated. The association between quantifiable MRI characteristics and macroscopic tissue damage at revision surgery has not been studied and therefore we believed it important to attempt to perform this analysis. Our conclusions

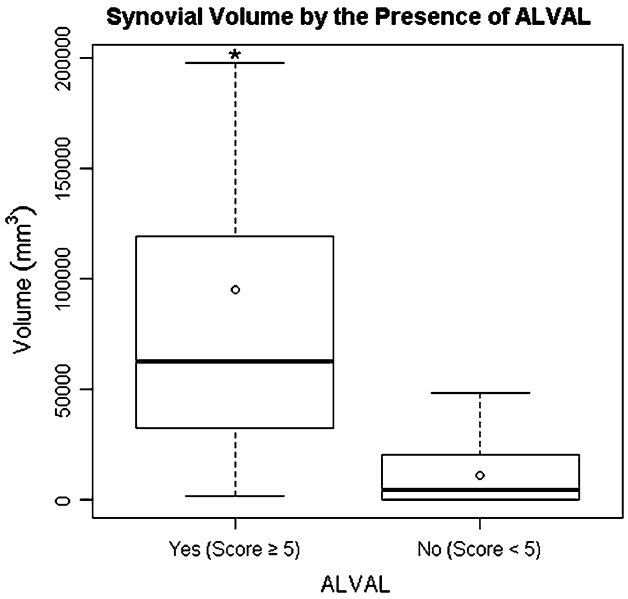

Fig. 7 A box plot shows the interquartile range (box edges representing 25th and 75th percentiles), median (band inside box), and mean (circle) for synovial volume by the presence of ALVAL. The error bars represent the minimum and maximum observed values within 1.5 times the interquartile range values. Outliers are not shown. The asterisk indicates a major difference in medians between outcome groups.

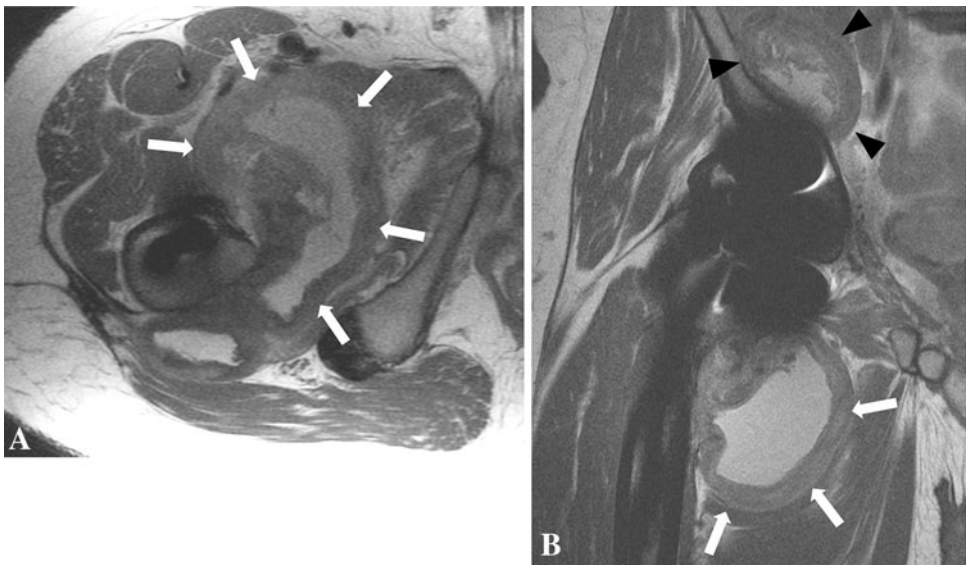

Fig. 8A–B (**A**) An axial (A) FSE image obtained after MOM THA in a 57-year-old man shows marked synovial expansion and thickening (white arrows) with anterior and posterior decompression. (**B**) The patient's coronal FSE image shows a large volume of synovitis decompressing inferiorly (white arrows) and superiorly into the subiliacus bursa (black arrowheads). The high volume of mixed-(fluid and solid) type synovitis combined with the greatly thickened synovial lining and disruption of the abductors resulting from distention of the pseudocapsule is suggestive of a high ALVAL score. This was confirmed at revision surgery with subsequent histologic analysis showing an ALVAL score of 9.

Table 2. Results of the comparison of MRI characteristics in patients with and without ALVAL

MRI characteristics investigated	Moderate-severe ALVAL (ALVAL ≥ 5) (N = 32 hips)	NonALVAL (ALVAL < 5) (N = 34 hips)	p value
Presence of synovitis (% yes)	100%	75%	0.002
Synovitis type (% mixed)	97%	25%	< 0.001
Median maximal synovial thickness (mm)	13.6	3.2	< 0.001
Median synovial volume (mm^3)	62,778	4540	< 0.001
Decompression of synovitis (% yes)	85%	41%	0.002
Low-signal intensity deposits (% yes)	59%	16%	0.003
Soft tissue edema (% yes)	62%	12%	< 0.001
Pseudocapsular dehiscence (% yes)	85%	44%	0.004
Presence of osteolysis (% yes)	29.1%	6.3 %	0.006
Neurovascular compression (% yes)	35%	6%	0.002
Abductor disruption (% yes)	62%	6%	0.004
Presence of nodes (% yes)	25%	8.8%	0.0276

Table 3. Results of the comparison of MRI characteristics in patients with severe versus none-mild tissue damage

MRI characteristics investigated	Severe damage (damage score ≥ 2) (N = 40 hips)	None-mild damage (damage score < 2) (N = 30 hips)	p value
Presence of synovitis (% yes)	100%	75%	0.001
Synovitis type (% mixed)	90%	29%	< 0.001
Median maximal synovial thickness (mm)	12.0	3.6	< 0.001
Median synovial volume (mm^3)	50,428	1988	< 0.001
Decompression of synovitis (% yes)	88%	32%	< 0.001
Low-signal intensity deposits (% yes)	63%	4%	< 0.001
Soft tissue edema (% yes)	55%	14%	0.007
Pseudocapsular dehiscence (% yes)	90%	32%	< 0.001
Presence of osteolysis (% yes)	31.5%	7.7%	0.0064
Neurovascular compression (% yes)	38%	0%	0.002
Abductor disruption (% yes)	53%	11%	0.001
Presence of nodes (% yes)	25%	6.7%	0.1083

on intraoperative tissue damage, however, are weakened by this limitation.

We found that maximal synovial thickness and synovial volume on MRI correlated with the ALVAL score. We also found that patients with an ALVAL score of 5 or greater were more likely to have a mixed pattern of synovitis (solid and fluid) with higher maximal synovial thicknesses and synovial volumes. These patients also were more likely to have decompression of synovitis, low signal intensity deposits, soft tissue edema, and pseudocapsule dehiscence. Finally, abductor disruption and neurovascular compression were more likely to be present on MRI in patients diagnosed with ALVAL. These findings are in contrast to recent MRI studies [10, 27] which found no distinguishing features between symptomatic and asymptomatic tissue lesions. A recent ultrasound study, however, did find that joint expansion and cystic and mass patterns on ultrasound were associated with symptomatic MOM hips [22].

Regarding tissue damage, we found that when comparing patients with a damage score of 2 or greater with patients with no or mild damage, the patients with severe tissue damage were more likely to have pseudocapsular dehiscence and a mixed pattern of synovitis with higher maximal synovial thickness and volume. The association between MRI characteristics and intraoperative tissue damage has not been studied previously. Our findings can provide the revision surgeon with vital preoperative clues regarding tissue damage and aid in formulating a plan in the presence of massive soft tissue defects.

The random forest predictive model used in this study provides us with an algorithm by which we can predict the outcomes for specific patients based on of the various MRI characteristics. This has advantages over a traditional scoring system in that the weights applied to each characteristic are dynamic. If a traditional MR scoring system was published, these scores would become static. Therefore, our institution favors designing a web-based screening tool such that the results of our random forest analysis can be updated in real time as new patients are added to the cohort. Our predictive model showed that maximal synovial thickness and a mixed synovial pattern were the two strongest predictors for detection of ALVAL. It also showed that pseudocapsule dehiscence, mixed

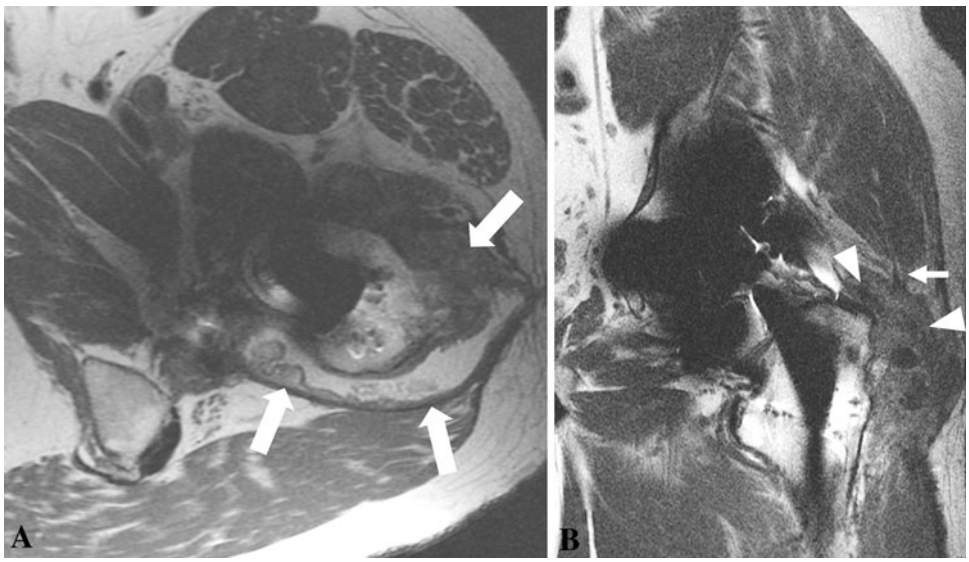

Fig. 9A–B (**A**) The axial FSE image obtained after a left MOM THA in a 46-year-old man shows synovial expansion and thickening with decompression of synovitis into the greater trochanteric bursa (white arrows) through a lateral dehiscence in the pseudocapsule. (**B**) The patient's coronal FSE image shows synovial expansion (white arrowheads) undermining the hip abductors with resulting disruption of the anterolateral fibers of the gluteus medius (small white arrow). The mixed-type synovial expansion with associated pseudocapsular dehiscence and extensive decompression of synovitis suggests substantial intraoperative damage. This is further supported by the large volume of synovitis and thick synovial lining. These findings were confirmed at revision surgery, when substantial soft tissue damage was seen and the patient received an intraoperative damage score of 3.

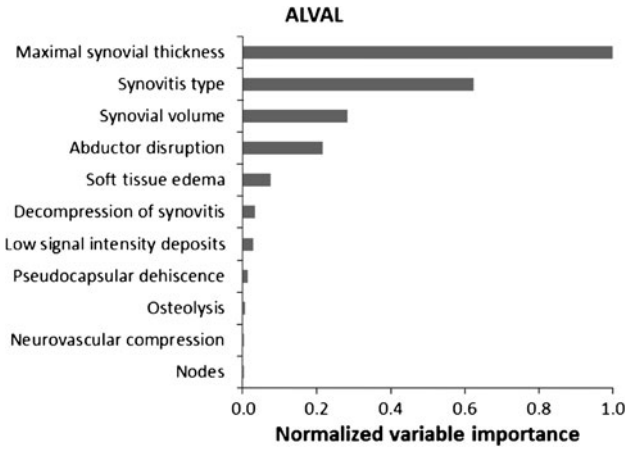

Fig. 10 A random forest analysis shows the normalized importance of MRI characteristics in predicting the presence of ALVAL. Importance is normalized to the best predictor, assigned the value of 1.

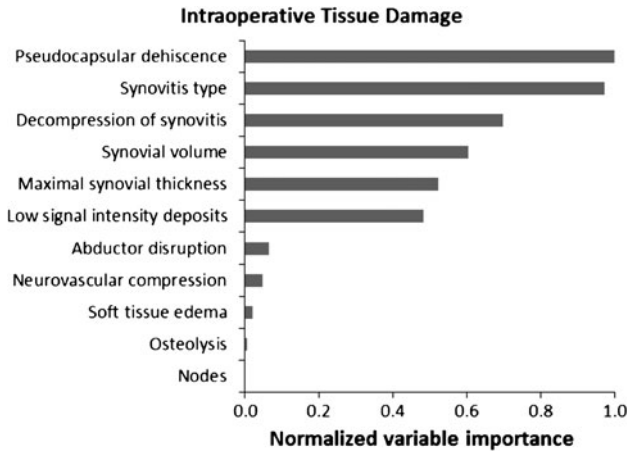

Fig. 11 A random forest analysis shows the normalized importance of MRI characteristics in predicting the presence of intraoperative tissue damage. Importance is normalized to the best predictor, assigned the value of 1.

pattern of synovitis, and decompression of synovitis were the strongest predictors of severe intraoperative tissue damage. These findings are in agreement with a recent study which concluded that consistency rather than the size of the pseudotumor is useful when predicting the likelihood for revision [11]. We found sensitivity and specificity of 94% and 87%, respectively, for detecting ALVAL and 90% and 86%, respectively, for quantifying tissue damage. These values are a major improvement on the predictive ability of blood cobalt and chromium ion levels for identifying a failing hip implant, which have sensitivity and specificity of 63% and 86%, respectively [9].

Other groups have used MRI to study soft tissue lesions around MOM hip implants, but none has used quantitative, reproducible MRI features and none has compared findings between groups formed on a histologic diagnosis [5, 8, 11, 27, 30, 35]. In a retrospective study, Toms et al. [30] qualitatively graded adverse reactions as mild, moderate, or severe and commented on features such as fluid or solid content and walls of the lesions. Hart et al. [10] proposed an MRI classification

for pseudotumors based on wall thickness, content, and shape. However, their study was limited by a small number of patients undergoing revision surgery and therefore correlation of MRI characteristics with histologic findings was not possible.

Modified MRI is a reproducible, noninvasive method to assess patients with a MOM hip implant. It has a strong predictive value in being able to detect an adverse tissue response in the form of ALVAL around a failed MOM hip arthroplasty and is also predictive of severe tissue damage. Maximal synovial thickness and synovial volume are quantifiable parameters that can be calculated on modified MRI and may be effective markers for surveillance of MOM hip arthroplasties. Further longitudinal study of asymptomatic hips is required to propose appropriate cut-off values beyond which revision surgery should be considered. Our observations suggest a mixed pattern of synovitis, with pseudocapsule dehiscence and decompression of synovitis, in the setting of large synovial volumes and synovial thicknesses may be an indication for early intervention in a MOM hip arthroplasty.

Acknowldgments We thank Alissa Burge MD for assistance with the MRI analysis, Matthew Koff PhD for help with the statistical analysis, and Giorgio Perino MD for grading the histologic samples.

Appendix

Appendix 1. Scoring sheet used to evaluate patients with a metal-on-metal hip arthroplasty

Metal-on-Metal MRI Score Sheet

Presence of Synovitis (Yes/No)
- If Yes:
  - Synovitis Type (Fluid, Solid, Mixed [fluid and solid])
  - Synovial Volume (mm^3) _____

Decompression of Synovitis (Yes/No)
- If Yes:
  - Decompression into Trochanteric Bursa (Yes/No)
  - Decompression into Iliopsoas Bursa (Yes/No)

Presence of Low Signal Intensity Deposits (Yes/No)
- If Yes:
  - Intracapsular (Yes/No)
  - Extracapsular (Yes/No)

Presence of Soft Tissue Edema (Yes/No)

Dehiscence of Pseudocapsule
- If Yes:
  - Posterior Dehiscence (Yes/No)
  - Anterior Dehiscence (Yes/No)

Osteolysis
- If Yes:
  - Femoral Osteolysis (Yes/No)
    - If Yes, Volume of Femoral Osteolysis (mm^3) _____
  - Periacetabular Osteolysis (Yes/No)
    - If Yes, Volume of Periacetabular Osteolysis (mm^3) _____

Loosening (Yes/No)
- If Yes:
  - Loosening of the Stem (Yes/No)
  - Loosening of the Cup (Yes/No)

Presence of Neurovascular Compression (Yes/No)
- If Yes:
  - Obturator Nerve Effected (Yes/No)
  - Sciatic Nerve Effected (Yes/No)
  - Femoral Nerve Effected (Yes/No)

Disruption of Abductors due to Distended Pseudocapsule (Yes/No)

Presence of Nodes (Yes/No)

References

1. Amstutz HC, Le Duff MJ, Campbell PA, Wisk LE, Takamura KM. Complications after metal-on-metal hip resurfacing arthroplasty. *Orthop Clin North Am*. 2011;42:207–230, viii.
2. Campbell P, Ebramzadeh E, Nelson S, Takamura K, De Smet K, Amstutz HC. Histological features of pseudotumor-like tissues from metal-on-metal hips. *Clin Orthop Relat Res*. 2010;468:2321–2327.
3. Coulter G, Young DA, Dalziel RE, Shimmin AJ. Birmingham hip resurfacing at a mean of ten years: results from an independent centre. *J Bone Joint Surg Br*. 2012;94:315–321.
4. Dorr LD, Wan Z, Longjohn DB, Dubois B, and Murken R. Total hip arthroplasty with use of the Metasul metal-on-metal articulation: four to seven-year results. *J Bone Joint Surg Am*. 2000;82:789–798.
5. Glyn-Jones S, Pandit H, Kwon YM, Doll H, Gill HS, Murray DW. Risk factors for inflammatory pseudotumour formation following hip resurfacing. *J Bone Joint Surg Br*. 2009;91:1566–1574.
6. Grammatopolous G, Pandit H, Kwon YM, Gundle R, McLardy-Smith P, Beard DJ, Murray DW, Gill HS. Hip resurfacings revised for inflammatory pseudotumour have a poor outcome. *J Bone Joint Surg Br*. 2009;91:1019–1024.
7. Hart AJ, Matthies A, Henckel J, Ilo K, Skinner J, Noble PC. Understanding why metal-on-metal hip arthroplasties fail: a comparison between patients with well-functioning and revised birmingham hip resurfacing arthroplasties. AAOS exhibit selection. *J Bone Joint Surg Am*. 2012;94:e22.
8. Hart AJ, Sabah S, Henckel J, Lewis A, Cobb J, Sampson B, Mitchell A, Skinner JA. The painful metal-on-metal hip resurfacing. *J Bone Joint Surg Br*. 2009;91:738–744.
9. Hart AJ, Sabah SA, Bandi AS, Maggiore P, Tarassoli P, Sampson B, Skinner JA. Sensitivity and specificity of blood cobalt and chromium metal ions for predicting failure of metal-on-metal hip replacement. *J Bone Joint Surg Br*. 2011;93:1308–1313.
10. Hart AJ, Satchithananda K, Liddle AD, Sabah SA, McRobbie D, Henckel J, Cobb JP, Skinner JA, Mitchell AW. Pseudotumors in association with well-functioning metal-on-metal hip prostheses: a case-control study using three-dimensional computed tomography and magnetic resonance imaging. *J Bone Joint Surg Am*. 2012;94:317–325.
11. Hauptfleisch J, Pandit H, Grammatopoulos G, Gill HS, Murray DW, Ostlere S. A MRI classification of periprosthetic soft tissue masses (pseudotumours) associated with metal-on-metal resurfacing hip arthroplasty. *Skeletal Radiol*. 2012;41:149–155.
12. Hayter CL, Koff MF, Shah P, Koch KM, Miller TT, Potter HG. MRI after arthroplasty: comparison of MAVRIC and conventional fast spin-echo techniques. *AJR Am J Roentgenol*. 2011; 197:W405–411.
13. Hing CB, Back DL, Bailey M, Young DA, Dalziel RE, Shimmin AJ. The results of primary Birmingham hip resurfacings at a mean of five years: an independent prospective review of the first 230 hips. *J Bone Joint Surg Br*. 2007;89:1431–1438.
14. Kwon YM, Glyn-Jones S, Simpson DJ, Kamali A, McLardy-Smith P, Gill HS, Murray DW. Analysis of wear of retrieved metal-on-metal hip resurfacing implants revised due to pseudotumours. *J Bone Joint Surg Br*. 2010;92:356–361.
15. Kwon YM, Ostlere SJ, McLardy-Smith P, Athanasou NA, Gill HS, Murray DW. "Asymptomatic" pseudotumors after metal-on-metal hip resurfacing arthroplasty: prevalence and metal ion study. *J Arthroplasty*. 2011;26:511–518.
16. Langton DJ, Jameson SS, Joyce TJ, Hallab NJ, Natu S, Nargol AV. Early failure of metal-on-metal bearings in hip resurfacing and large-diameter total hip replacement: a consequence of excess wear. *J Bone Joint Surg Br*. 2010;92:38–46.
17. Langton DJ, Joyce TJ, Jameson SS, Lord J, Van Orsouw M, Holland JP, Nargol AV, De Smet KA. Adverse reaction to metal debris following hip resurfacing: the influence of component type, orientation and volumetric wear. *J Bone Joint Surg Br*. 2011;93:164–171.
18. Long WT, Dorr LD, Gendelman V. An American experience with metal-on-metal total hip arthroplasties: a 7-year follow-up study. *J Arthroplasty*. 2004;19(8 suppl 3):29–34.
19. Matthies AK, Skinner JA, Osmani H, Henckel J, Hart AJ. Pseudotumors are common in well-positioned low-wearing metal-on-metal hips. *Clin Orthop Relat Res*. 2012;470:1895–1906.
20. Meneghini RM, Hallab NJ, Jacobs JJ. Evaluation and treatment of painful total hip arthroplasties with modular metal taper junctions. *Orthopedics*. 2012;35:386–391.
21. Mesaros S, Rocca MA, Kacar K, Kostic J, Copetti M, Stosic-Opincal T, Preziosa P, Sala S, Riccitelli G, Horsfield MA, Drulovic J, Comi G, Filippi M. Diffusion tensor MRI tractography and cognitive impairment in multiple sclerosis. *Neurology*. 2012; 78:969–975.
22. Nishii T, Sakai T, Takao M, Yoshikawa H, Sugano N. Ultrasound screening of periarticular soft tissue abnormality around metal-on-metal bearings. *J Arthroplasty*. 2012;27:895–900.
23. Ollivere B, Darrah C, Barker T, Nolan J, Porteous MJ. Early clinical failure of the Birmingham metal-on-metal hip resurfacing is associated with metallosis and soft-tissue necrosis. *J Bone Joint Surg Br*. 2009;91:1025–1030.
24. Pandit H, Glyn-Jones S, McLardy-Smith P, Gundle R, Whitwell D, Gibbons CL, Ostlere S, Athanasou N, Gill HS, Murray DW. Pseudotumours associated with metal-on-metal hip resurfacings. *J Bone Joint Surg Br*. 2008;90:847–851.
25. Potter HG, Foo LF. Magnetic resonance imaging of joint arthroplasty. *Orthop Clin North Am*. 2006;37:361–373, vi–vii.
26. Potter HG, Nestor BJ, Sofka CM, Ho ST,. Peters LE, Salvati EA. Magnetic resonance imaging after total hip arthroplasty: evaluation of periprosthetic soft tissue. *J Bone Joint Surg Am*. 2004; 86:1947–1954.
27. Sabah SA, Mitchell AW, Henckel J, Sandison A, Skinner JA, Hart AJ. Magnetic resonance imaging findings in painful metal-on-metal hips: a prospective study. *J Arthroplasty*. 2011;26:71–76, 76.e1–2.
28. Schmalzried TP. Metal-metal bearing surfaces in hip arthroplasty. *Orthopedics*. 2009; 32: doi:10.3928/01477447-20090728-06.
29. Suh JS, Jeong EK, Shin KH, Cho JH, Na JB, Kim DH, Han CD. Minimizing artifacts caused by metallic implants at MR imaging: experimental and clinical studies. *AJR Am J Roentgenol*. 1998; 171:1207–1213.
30. Toms AP, Marshall TJ, Cahir J, Darrah C, Nolan J, Donell ST, Barker T, Tucker JK. MRI of early symptomatic metal-on-metal total hip arthroplasty: a retrospective review of radiological findings in 20 hips. *Clin Radiol*. 2008;63:49–58.
31. Treacy RB, McBryde CW, Shears E, Pynsent PB. Birmingham hip resurfacing: a minimum follow-up of ten years. *J Bone Joint Surg Br*. 2011;93:27–33.
32. Walde TA, Weiland DE, Leung SB, Kitamura N, Sychterz CJ, Engh CA Jr, Claus AM, Potter HG, Engh CA Sr. Comparison of CT, MRI, and radiographs in assessing pelvic osteolysis: a cadaveric study. *Clin Orthop Relat Res*. 2005;437:138–144.
33. Willert HG, Buchhorn GH, Fayyazi A, Flury R, Windler M, Koster G, Lohmann CH. Metal-on-metal bearings and hypersensitivity in patients with artificial hip joints: a clinical and histomorphological study. *J Bone Joint Surg Am*. 2005;87:28–36.
34. Williams DH, Greidanus NV, Masri BA, Duncan CP, Garbuz DS. Prevalence of pseudotumor in asymptomatic patients after metal-on-metal hip arthroplasty. *J Bone Joint Surg Am*. 2011;93:2164–2171.
35. Wynn-Jones H, Macnair R, Wimhurst J, Chirodian N, Derbyshire B, Toms A, Cahir J. Silent soft tissue pathology is common with a modern metal-on-metal hip arthroplasty. *Acta Orthop*. 2011;82: 301–307.